

## Studies of the beta dependence of transport in ASDEX Upgrade

L. Vermare, F. Ryter, J. Stober, C. Angioni, R. Bilato, L. Horton,

B. Kurzan, C.F. Maggi, H. Meister, J. Schirmer and ASDEX Upgrade Team

*Max-Planck-Institut für Plasmaphysik, EURATOM Association, D-85748 Garching, Germany*

### Introduction

Particle and heat transport induced by micro-turbulence plays a crucial role in tokamak performances. Comparisons between tokamak experiments and theory and predictions of transport in future devices, including ITER, rely on the knowledge of transport dependencies on dimensionless parameters such as the normalized toroidal Larmor radius  $\rho^*$ , the normalized collisionality  $\nu^*$  and the normalized plasma pressure  $\beta$ . In particular, the  $\beta$  dependence of transport is an indication of purely electrostatic (no dependence) or electromagnetic nature of plasma turbulence. At present, effects of  $\beta$  are not completely understood. Global analysis using scaling laws shows a strong degradation of the energy confinement time  $\tau_E$  with increasing  $\beta$  ( $B\tau_E \propto \beta^{-0.9}$  [1]). However, dedicated experiments on DIII-D [2] and JET [3] exhibit a very weak  $\beta$  dependence in the energy confinement time and heat transport coefficients while recent experiments in JT-60U yield a degradation of  $\tau_E$  with  $\beta$  [4]. To contribute to clarify this discrepancy, investigations on the  $\beta$  dependence of transport on ASDEX Upgrade have been started.

### Experimental setup

Dedicated  $\beta$  scan experiments are performed while keeping  $\rho^*$ ,  $\nu^*$ , the safety factor  $q$  and the plasma shape constant. Therefore, the magnetic field  $B$  is varying and the plasma parameters need to satisfy the relationships:  $I \propto B$ ;  $n \propto B^4$ ;  $T \propto B^2$ . Following these requests,  $\beta$  varies as  $\propto B^4$ . Assuming that the energy confinement time can be written as  $B\tau_E \propto \beta^{\alpha_\beta} F(\rho^*, \nu^*, \dots)$ , the heating power must vary as  $P_h \propto B^{7-4\alpha_\beta}$ . Experimentally, the  $\beta$  range is limited by the L-H transition at low  $\beta$  and by the MHD limit at high  $\beta$ . In addition, as density has to vary as  $\beta$  ( $\propto B^4$ ) other limitations come from the natural density and the Greenwald limit. In the work presented here, two separate  $\beta$  scans in H-mode with Type-I ELMs between  $\beta_N = [1.4 - 2.2]$  and  $\beta_N = [1.4 - 2]$  covering different density ranges have been performed in ASDEX Upgrade. For all these experiments a single-null divertor plasma configuration was used with a moderate triangularity ( $\delta = 0.2$ ) and  $q_{95} = 3.8$ . These Deuterium plasmas were heated by neutral beam injection (NBI) and in some cases with (H-minority) ICRH heating. The voltage of NBI injectors was adjusted according to the density to match as much as possible the heating deposition profile between low and high- $\beta$  discharges. Equilibria and q-profiles are reconstructed using the equilibrium code CLISTE. NBI and ICRH heating deposition profiles are calculated

respectively by the Monte-Carlo FAFNER and the TORIC codes. Parameters of both scans are summarized in the following table. The differences between scans is the density and the use of ICRH during the first scan.

	scan1				scan2	
pulse	20989	21101	21225	21226	21403	21426
B(T)	-2.10	-2.29	-2.28	-2.28	-2.12	-2.33
I(MA)	1.00	1.10	1.09	1.09	0.99	1.09
$\bar{n}_e(10^{19}m^{-3})$	7.03	7.82	8.13	8.40	4.64	7.59
$P_{NBI}(MW)$	2.4	7.75	7.5	10	2.6	8.75
$P_{ICRH}(MW)$	1.11	0.6	3.8	3.8	0	0
$q_{95}$	3.8	3.9	3.8	3.8	3.8	3.8
a/R	0.30	0.31	0.30	0.30	0.30	0.30
$\kappa$	1.84	1.79	1.84	1.83	1.82	1.86
$\delta$	0.21	0.24	0.22	0.23	0.20	0.22
$\rho^*(10^{-3})$	6.1	6.9	6.6	6.7	7.0	7.1
$v^*$	0.610	0.300	0.396	0.388	0.243	0.279
$\beta_N$	1.41	2.22	1.97	2.22	1.41	2.05
$\beta_{th}$	1.32	2.07	1.87	2.09	1.30	1.93
$B\tau_{th}$	0.284	0.217	0.155	0.138	0.342	0.208

### Global analysis

The normalized thermal energy confinement times  $B\tau_{th}$  of the six discharges are presented in the figure 1. For each scan, there is a clear degradation of the global confinement with increasing  $\beta$ . The first scan (blue) is composed of one low  $\beta$  discharge (20989) and 3 high  $\beta$  discharges (21101, 21225 and 21226). The  $\beta$  dependence of  $B\tau_{th}$  vary significantly between each pair :  $\alpha_\beta = -0.6 \pm 0.4$  ;  $-1.7 \pm 0.9$  and  $-1.5 \pm 0.6$  from the low- $\beta$  discharge 20989 to respectively the high- $\beta$  discharge 21101, 21225 and 21226. Indeed, the heating deposition profiles are strongly off-axis for the discharges 21225 and 21226. In addition, it was not possible to reach the required high density and high  $\beta$  simultaneously. From

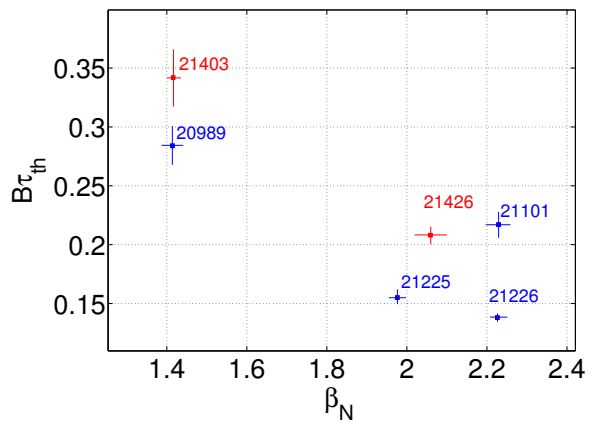


Figure 1: Normalized thermal energy confinement time as a function of normalized  $\beta$ .

previous experiments performed on different devices it have been found that  $B\tau_{th}$  varies as  $\rho^{*-3}$  which correspond to the Gyro-Bohm scaling and as  $v^{*-0.3}$  at low density and as  $v^{*-1}$  at higher density [6, 5]. Therefore,  $\rho^*$  and  $v^*$  mismatching induce errors in  $\beta$  dependence of  $\tau_{th}$  which can be corrected. Applying a correction as  $\rho^{*-3}v^{*-1}$  to compensate the mismatching, the  $\beta$  dependencies obtained between 20989 and respectively 21101, 21225 and 21226 discharge change to  $\alpha_\beta = -1, -1.9$  and  $-1.5$ . For these last pair,  $\alpha_\beta$  does not differ from the uncorrected result because the  $\rho^*$  and  $v^*$  corrections cancel each other. The second scan (red) was easier to perform because of the lower density. Therefore, the  $\rho^*$  and  $v^*$  matching are better than the in first scan. However it also shows a  $\beta$  dependence as  $B\tau_{th} \propto \beta_{th}^{-1.2 \pm 0.7}$ . The corrections for mismatch lead to  $\alpha_\beta = -0.58$  for  $\rho^{*-3}v^{*-1}$  and  $\alpha_\beta = -0.94$  for  $\rho^{*-3}v^{*-0.3}$ . The  $v^*$  mismatching has opposite sign than in the first scan which explain that the  $\alpha_\beta$  decreases applying the corrections for this pair while it was increased in the previous case. Finally, with or without mismatching corrections, the trend of the global analysis indicate a significative and negative  $\beta$  dependence.

### Local analysis

The local transport studies are presented for the second scan for which the  $\rho^*$  and  $v^*$  profiles are better matched (figures 2a and 2b). The  $\rho^*$  mismatching is lower than 10% but the  $v^*$  mis-

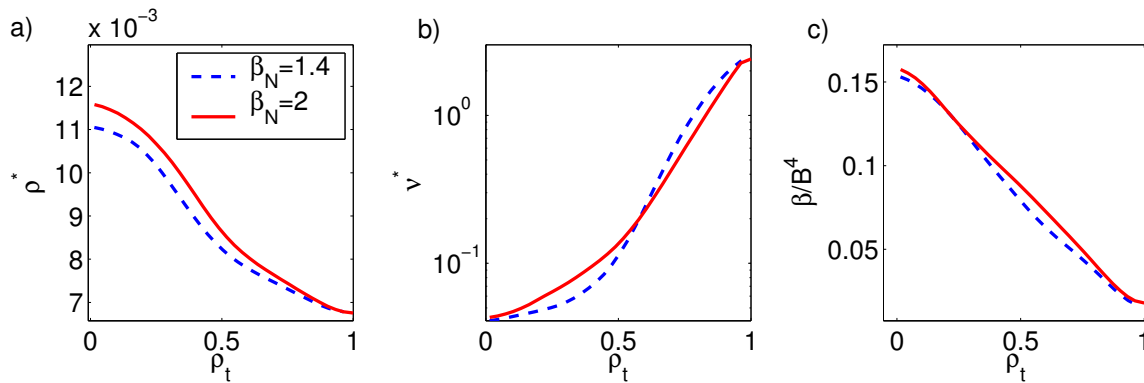


Figure 2:  $\rho^*$  a),  $v^*$  b) and normalized  $\beta$  c) profiles for the discharges 21403@3.1s and 21426@3.8s.

matching reaches 30% locally. The matching of the  $\beta_{th}/B^4$  profile is good from the edge to the center (figure 2c). The effective heat diffusivities,  $\chi_{eff} = (q_e + q_i)/(n_e \nabla T_e + n_i \nabla T_i)$ , from power balance analysis using the ASTRA code are presented in figure 3. The error-bars (systematic and random) take into account the uncertainties in the temperature gradients ( $\Delta\rho_t = 0.4$ ) and in the density profile. Comparatively, uncertainties on the total flux can be neglected. Gradients uncertainties were evaluated by varying the temperature profiles within their error-bars (around 15%

for  $T_e$  and 10% for  $T_i$ ). The error-bars on  $\chi_{eff}$  are typically around 25%. The normalized  $\chi_{eff}$  is higher in the high- $\beta$  discharge. Even if the difference is within the local error bars, the tendency shows an augmentation of transport with increasing  $\beta$  on a large radial area ( $\rho_t = 0.3-0.8$ ). The  $\beta$  dependence of  $\chi_{eff}$  varies with  $\rho_t$  and reaches a maximum dependence as  $\chi_{eff}/B \propto \beta^1$  at  $\rho_t = 0.5$ . Average from  $\rho_t = 0.3$  to  $\rho_t = 0.7$  gives  $\chi_{eff}/B \propto \beta^{0.7}$ .

## Conclusion

These first investigations on the  $\beta$  dependence of transport in ASDEX-Upgrade show a degradation of the confinement time with increasing  $\beta$ . Coherently, local analysis yields an enhancement of the effective heat diffusivity with  $\beta$ . However, during these experiments the  $v^*$  and the heating deposition profiles are not perfectly matched. Attempts to correct the  $v^*$  mismatch did not cancel the strong negative  $\beta$  dependence of the confinement time. The global confinement degradation found in ASDEX Upgrade as  $B\tau_{th} \propto \beta^{-1.2 \pm 0.7}$  leads to  $B\tau_{th} \propto \beta^{-0.9}$  with  $\rho^*$  and  $v^*$  mismatching corrections. These both dependencies are in agreement with the  $\beta$  exponents derived from the ITER-IPB98(y,2) scaling law and with the recent experiments performed in JT-60U which yield a  $\beta$  dependence as  $B\tau_{th} \propto \beta^{-0.6}$  [4]. But the strong discrepancy with experiments carried out in DIII-D and JET where no  $\beta$  dependence on both energy confinement time and local diffusivity have been found still needs to be clarified. The higher collisionality in ASDEX Upgrade experiments and the plasma shape, in particular the upper triangularity could play a role.

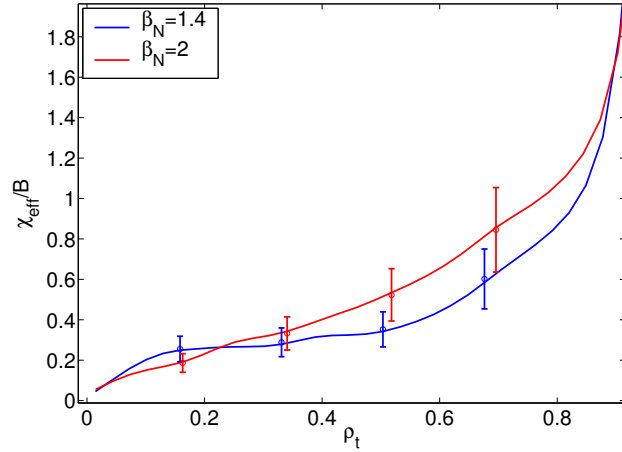


Figure 3: Radial profiles of the effective thermal diffusivity, normalized to the scaling of the Bohm diffusion coefficient.

## References

- [1] ITER Physics Basis, Nuclear Fusion **39**, 2175 (1999)
- [2] C.C. Petty, T.C. Luce, D.C. McDonald and al., Physics of Plasma **11**, 5 (2004)
- [3] D.C. McDonald and al., Plasma Phy. and Control. Fusion **46**, A-215-A-225 (2004)
- [4] H. Urano, T. Tkizuaka and al., to be published in Nuclear Fusion (2006)
- [5] M. Greenwald and al., Plasma Phy. and Control. Fusion **40**, 789-792 (1998)
- [6] J. G. Cordey, D. C McDonald and al., Proc. 31st EPS Conf. on Contr. Fusion and Plasma Physics, London ECA Vol.28G, O-1.05 (2004)